J|A|C|S ARTICLES

Published on Web 11/06/2009

Reversed Enantioselectivity of Diisopropyl Fluorophosphatase against Organophosphorus Nerve Agents by Rational Design

Marco Melzer,[†,‡] Julian C.-H. Chen,[§] Anne Heidenreich,[†] Jürgen Gäb,[†,⊥] Marianne Koller,[∥] Kai Kehe,[∥] and Marc-Michael Blum*[,†]

Blum-Scientific Services, Ledererstrasse 23, 80331 Munich, Germany, Institute of Biophysical Chemistry, Goethe University Frankfurt, Max-von-Laue-Strasse 9, 60438 Frankfurt, Germany, Bundeswehr Institute of Pharmacology and Toxicology, Neuherbergstrasse 11, 80937 Munich, Germany, Institute of Pathology, Johannes Gutenberg University Mainz, 55101 Mainz, Germany, and Institute of Pharmaceutical Chemistry, Philipps University Marburg, 35032 Marburg, Germany

Received July 2, 2009; E-mail: mmblum@blum-scientific.de

Abstract: Diisopropyl fluorophosphatase (DFPase) from *Loligo vulgaris* is an efficient and robust biocatalyst for the hydrolysis of a range of highly toxic organophosphorus compounds including the nerve agents sarin, soman, and cyclosarin. In contrast to the substrate diisopropyl fluorophosphate (DFP) the nerve agents possess an asymmetric phosphorus atom, which leads to pairs of enantiomers that display markedly different toxicities. Wild-type DFPase prefers the less toxic stereoisomers of the substrates which leads to slower detoxification despite rapid hydrolysis. Enzyme engineering efforts based on rational design yielded two quadruple enzyme mutants with reversed enantioselectivity and overall enhanced activity against tested nerve agents. The reversed stereochemical preference is explained through modeling studies and the crystal structures of the two mutants. Using the engineered mutants in combination with wild-type DFPase leads to significantly enhanced activity and detoxification, which is especially important for personal decontamination. Our findings may also be of relevance for the structurally related enzyme human paraoxonase (PON), which is of considerable interest as a potential catalytic *in vivo* scavenger in case of organophosphorus poisoning.

Introduction

Enzyme engineering, through methods such as site-directed, site-saturation mutagenesis, and directed evolution are common ways of improving upon and augmenting an enzyme's activity.[1−3] Engineering stereoselectivity into an enzyme has potential applications in enzyme-assisted chemical synthesis and creation of novel unnatural compounds and drug leads. The enzyme diisopropyl fluorophosphatase (DFPase, EC 3.1.8.2) from the squid *Loligo vulgaris* is a potent and well characterized phosphotriesterase capable of hydrolyzing a variety of organophosphorus compounds that act as irreversible inhibitors of acetylcholinesterase (AChE). Substrates include diisopropyl fluorophosphate (DFP) and a range of highly toxic G-type organophosphorus (OP) nerve agents such as sarin (GB), soman (GD), and cyclosarin (GF) that still pose a credible threat to military personnel as well as civilian populations (Scheme 1).[4−7]

Scheme 1. Structures of DFP and Organophosphorus Nerve Agents and Hydrolysis of DFP Catalyzed by DFPase with Reaction Products[a]

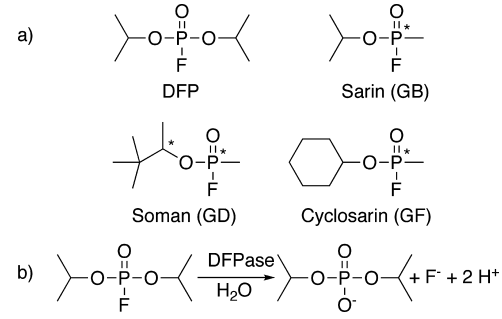

[a] (a) Structures of DFP and organophosphorus nerve agents, which are substrates of DFPase. Asterisks indicate stereocenters. (b) Hydrolysis of DFP catalyzed by DFPase with reaction products.

While DFP is achiral, the nerve agents possess a stereocenter at the phosphorus atom and exist as pairs of enantiomers (four stereoisomers for GD due to an additional stereocenter in the

[†] Blum-Scientific Services.
[‡] J. Gutenberg University Mainz.
[§] Goethe University Frankfurt.
[⊥] Philipps University Marburg.
[∥] Bundeswehr Institute of Pharmacology and Toxicology.

(1) Toscano, M. D.; Woycechowsky, K. J.; Hilvert, D. *Angew. Chem., Int. Ed.* **2007**, *46*, 3212–3236.
(2) Penning, T. M.; Jez, J. M. *Chem. Rev.* **2001**, *101*, 3027–3046.
(3) Antikainen, N. M.; Martin, S. F. *Bioorg. Med. Chem.* **2005**, *13*, 2701–2716.
(4) Scharff, E. I.; Koepke, J.; Fritzsch, G.; Lücke, C.; Rüterjans, H. *Structure (Cambridge, MA, U.S.)* **2001**, *9*, 493–502.
(5) Blum, M. M.; Löhr, F.; Richardt, A.; Rüterjans, H.; Chen, J. C. H. *J. Am. Chem. Soc.* **2006**, *128*, 12750–12757.
(6) Blum, M. M.; Timperley, C. M.; Williams, G. R.; Thiermann, H.; Worek, F. *Biochemistry* **2008**, *47*, 5216–5224.
(7) Blum, M. M.; Mustyakimov, M.; Rüterjans, H.; Kehe, K.; Schoenborn, B. P.; Langan, P.; Chen, J. C. H. *Proc. Natl. Acad. Sci. U.S.A.* **2009**, *106*, 713–718.

10.1021/ja905444g CCC: $40.75

pinacolyl side chain). These optical isomers also exhibit different inhibitory potencies toward acetylcholinesterase (AChE) and therefore different toxicities[8] and can racemize in aqueous solution[9] in a fluoride catalyzed process.

Earlier work revealed that wild-type (WT) DFPase shows a stereochemical preference for the less toxic enantiomers of G-type nerve agents.[10] While this is not a large concern for the decontamination of equipment as long as full detoxification is achieved within a certain time, it is a problem for applications requiring a rapid decrease in toxicity, such as topical applications or *in vivo* use. At the same time a very high enantioselectivity of the enzyme, as normally required for enzymes used in organic synthesis,[11,12] is also not desirable as complete hydrolysis of the agent is still required. Therefore, the goal is an enzyme mutant with enhanced total activity, that displays enantioselectivity for the more toxic stereoisomer leading to a rapid decrease in toxicity while still turning over the less toxic stereoisomer rapidly enough to ensure complete hydrolysis.

The currently proposed mechanism for DFPase assumes that the incoming substrate replaces a water molecule in the coordination sphere of the active site calcium ion binding via its phosphoryl group and is activated for nucleophilic attack by the free oxygen atom of calcium-coordinating amino acid residue D229. This results in the formation of a phosphoenzyme intermediate, which is subsequently hydrolyzed to form a phosphonic or phosphoric acid as the reaction product.[5] This mechanism has been supported by the results obtained with OP-compounds with fluorogenic leaving groups as substrates[6] and by the solvent orientation and protonation states found in a recent neutron diffraction study.[7] The phosphotriesterase activity of paraoxonase 1 (PON1) might follow the same mechanism,[5,6] a claim that has been supported by a recent *in silico* study.[13] Like DFPase, PON1 preferably hydrolyzes the less toxic nerve agent stereoisomers.[14−16] In order to find PON1 mutants with reversed or broader stereoselectivity, directed evolution was used employing nerve agent derivatives with fluorogenic leaving groups.[17,18]

Realizing the complications arising from the different size and chemical behavior of chromogenic or fluorogenic leaving groups compared to the small fluoride leaving group found in the original substrates, our approach focused on the original substrates accepting that a high-throughput assay would not be available for the screening of large mutant libraries and that further restrictions would arise due to the high toxicity of the substrates. With an atomic resolution X-ray[19] and a neutron[7] structure of DFPase available, combined with knowledge about the phosphotriesterase mechanism,[5] we aimed to create improved mutants using rational design. Furthermore, the high stability of the enzyme and the rigidity of the active site pocket make DFPase an attractive candidate for these re-engineering studies. In this work we report the creation of DFPase mutants with reversed stereoselectivity and enhanced activity against a range of nerve agent substrates by rational design and explain the changed stereochemical preference by structural analysis and computer modeling.

Materials and Methods

Substrates. Chemical warfare agents were made available by the German Ministry of Defense and handled in accordance with the Chemical Weapons Convention. DFP was obtained from Fluka. Organophosphorus compounds were used as approximately 2% (v/v) stock solutions in dry acetonitrile.

Expression and Purification of DFPase. Wild-type DFPase and mutants were expressed in *E. coli* BL21 cells and purified according to the method of Hartleib and Rüterjans.[20] Mutants were generated by site-directed mutagenesis. Detailed procedures are described in the Supporting Information.

Crystallization and Structure Determination. Crystals of DFPase mutants were grown at room temperature (RT) by vapor diffusion using the hanging drop method. A 2 μL portion of 1 mM protein solution (ca. 35 mg/mL) was mixed with well solution containing 0.1 M Tris buffer pH 8.5, 2% tacsimate, 16% PEG 3350 for mutant E37A/Y144A/R146A/T195M (Mut1), or 0.2 M KCl, 0.05 M HEPES buffer pH 7.5, 35% pentaerythriol propoxylate (5/4 PO/OH) for mutant E37D/Y144A/R16A/T195M (Mut2). Crystals grew over a period of 2−4 weeks and were transferred to cryoprotectant containing mother liquor with 20% glycerol and flash-frozen in liquid nitrogen prior to data acquisition.

Data was collected at 100 K at ESRF beamlines ID14−1 (Mut1) and BM16 (Mut2). Data were integrated, reduced, and scaled with MOSFLM/SCALA (Mut1) and HKL2000 (Mut2).[21,22] Molecular replacement was done using the RT WT structure of DFPase (PDB: 2GVW) excluding the waters and the two calcium ions, with alanines in place of the mutated residues. For Mut2, rotation and translation searches were performed in MOLREP,[23] yielding an unambiguous set of solutions corresponding to the four molecules in the asymmetric unit. Mut1 maps were calculated using difference Fourier maps, clearly showing the amino acid differences at residue 37 between Mut1 and Mut2. Manual building in Coot[24] was followed by rounds of positional, individual B-factor, and simulated annealing refinement in CNS 1.2[25] to yield the final refined structures.

Kinetic Measurements. Specific enzymatic activities and kinetic parameters were recorded using Fourier transform infrared (FTIR) spectroscopy according to the method of Gäb et al.[26] To discrimi-

(8) Benschop, H. P.; De Jong, L. P. A. *Acc. Chem. Res.* **1988**, *21*, 368–374.
(9) Christen, P. J.; van den Muysenberg, J. A. *Biochim. Biophys. Acta* **1965**, *110*, 217–220.
(10) Schulz, W.; Schäfer, B.; Stroop, G.; Rüterjans, H. *Forschungsberichte aus der Wehrtechnik* **1987**, T/R770/D 00001/D 1750.
(11) Bornscheuer, U. T.; Pohl, M. *Curr. Opin. Chem. Biol.* **2001**, *5*, 137–143.
(12) Faber, K. *Biotransformations in Organic Chemistry*, 4th ed.; Springer-Verlag: Berlin, Germany, 1999.
(13) Hu, X.; Jiang, X.; Lenz, D. E.; Cerasoli, D. M.; Wallquist, A. *Proteins* **2009**, *75*, 486–498.
(14) Amitai, G.; Gaidukov, L.; Adani, R.; Yishay, S.; Yacov, G.; Kushnir, M.; Teitlboim, S.; Lindenbaum, M.; Bel, P.; Kerhsonsky, O.; Tawfik, D. S.; Meshulam, H. *FEBS J.* **2006**, *273*, 1906–1919.
(15) Yeung, D. T.; Smith, J. R.; Sweeney, R. E.; Lenz, D. E.; Cerasoli, D. M. *FEBS J.* **2007**, *274*, 1183–1191.
(16) Yeung, D. T.; Smith, J. R.; Sweeney, R. E.; Lenz, D. E.; Cerasoli, D. M. *J. Anal. Toxicol.* **2008**, *32*, 86–91.
(17) Amitai, G.; Adani, R.; Yakov, G.; Yishay, S.; Teitlboim, S.; Tveria, L.; Limanovich, O.; Kushnir, M.; Meshulam, H. *Toxicology* **2007**, *233*, 187–198.
(18) Amitai, G.; Adani, R.; Limanovich, O.; Teitlboim, S.; Yishay, S.; Tveria, L.; Yacov, G.; Meshulam, H.; Raveh, L. *Chem. Biol. Interact.* **2008**, *175*, 249–254.
(19) Koepke, J.; Scharff, E. I.; Lücke, C.; Rüterjans, H.; Fritzsch, G. *Acta Crystallogr., Sect. D: Biol. Crystallogr.* **2003**, *59*, 1744–1754.
(20) Hartleib, J.; Rüterjans, H. *Protein Expression Purif.* **2001**, *21*, 210–219.
(21) Leslie, A. G. W. *Jnt CCP4/ESF-EACBM Newsl. Protein Crystallogr.* **1992**, *26*, 27–33.
(22) Otwinowsky, Z.; Minor, W. *Methods Enzymol.* **1997**, *276*, 307–326.
(23) Vagin, A.; Teplyakov, A. *J. Appl. Crystallogr.* **1997**, *30*, 1022–1025.
(24) Emsley, P.; Cowtan, K. *Acta Crystallogr., Sect. D: Biol. Crystallogr.* **2004**, *60*, 2126–2132.
(25) Brunger, A. T.; Adams, P. D.; Clore, G. M.; DeLano, W. L.; Gros, P.; Grosse-Kunstleve, R. W.; Jiang, J. S.; Kuszewski, J.; Nilges, M.; Pannu, N. S.; Read, R. J.; Rice, L. M.; Simonson, T.; Warren, G. L. *Acta Crystallogr., Sect. D: Biol. Crystallogr.* **1998**, *54*, 905–921.
(26) Gäb, J.; Melzer, M.; Kehe, K.; Richardt, A.; Blum, M. M. *Anal. Biochem.* **2009**, *385*, 187–193.

nate the hydrolysis rates for the different stereoisomers of the chiral substrates we used a combination of two methods. The overall (racemic) hydrolysis rate was measured titrimetrically using a pH-Stat method[27] while the hydrolysis of the toxic stereoisomer was determined by the inhibitory potency of the reaction solution against AChE. Human hemoglobin-free erythrocyte ghosts were used as the AChE source.[28] Samples were taken at intervals, and the reaction was quenched in formate buffer (pH 3.5). The inhibitory potency and therefore the concentration of the toxic stereoisomer were determined by a modified Ellman assay using acteylthiocholine and DTNB.[29−31] Concentrations were calculated using the method of Hart and O'Brien.[32] Detailed procedures are described in the Supporting Information.

k_{cat}/K_M values for the enantiomers of GB and GF were determined by modifying a mathematical procedure described by Yeung et al.[15] for analyzing kinetic data for the four stereoisomers of GD. In the presence of a racemic mixture of GB or GF, the catalyzed reaction is analogous to simultaneously deriving the kinetic constants for the hydrolysis of two competitive substrates. Instead of fitting the individual values of k_{cat} and K_M for the two enantiomers (four variables), only k_{cat}/K_M values (two variables) were used for the fitting procedure, which was carried out using the software MATHEMATICA. This was due to the fact that all reactions with GB and GF were carried out at nonsaturating conditions.

Chiral GC/MS. The GC/MS method for the separation of cyclosarin enantiomers was based on the original method of Reiter et al.[33] with some modifications. The GC/MS system consisted of a 6890N gas chromatograph connected to a 5973 Network MS (both Agilent Technologies) equipped with a cold injection system (CIS). According to the original method the CIS was operated in the solvent vent mode at 50 °C for 1.8 min with the split exit open. After this initialization, the split exit was closed and the temperature was raised to 260 °C using the maximal heating rate. After the temperature was reached, the split exit was opened again and the liner was purged for 3 min with carrier gas (purified helium passed over moisture, oxygen, and two active charcoal filters) with a flow rate of 1.3 mL/min. The oven program was initiated at 50 °C holding the temperature for 2 min. The temperature was then raised to 105 °C with a rate of 40 °C/min (no hold), then further to 130 °C at a rate of 3 °C/min (no hold), and finally to 170 °C at a rate of 40 °C/min (no hold). The MS was operated in the selected ion-monitoring mode (SIM) with a dwell-time of 100 ms for *m*/*z* 99. The enantiomers of cyclosarin were separated using a chiral GAMMADEX 225 column (Supelco, 30 m length, 0.25 i.d., 25 μm film-thickness). Sample preparation was carried out using solid phase extraction (SPE). Cyclohexyl columns (Isolute) were conditioned using 1 mL methanol followed by 1 mL water and loaded with 10 μL of sample solution afterward. After being washed with water (3 × 1 mL) cyclosarin was eluted with 1 mL of isopropanol and diluted 10-fold using the same solvent in an autosampler vial for GC/MS determination.

Docking. Docking experiments were carried out using AutoDock4[34] in combination with the AutoDock-Tools[35] GUI. A gridbox (50 × 50 × 50 points with a grid spacing of 0.375 Å) was placed over the binding site of the protein and centered slightly above the catalytic calcium ion. The Lamarckian genetic algorithm with a maximum of 20 million energy evaluations in combination with a local search algorithm was used for each of the 100 individual docking runs. All other parameters were left to the preset values in AutoDock-Tools. Low energy conformers of the ligands were obtained with the CORINA program.[36]

Modeling. Models of the phosphoenzyme intermediate were generated by hand using Coot[24] and subjected to thorough energy minimization using both the steepest descent and conjugate gradient algorithm as implemented in the GROMACS[37,38] simulation software. Modifications of the GROMOS96 43a1 force field[39] for the phosphorlyated aspartate residues were carried out on the basis of the results of the PRODRG[40] server for these modified amino acids.

Results

Stereochemical Preference of WT DFPase. In a first step the stereochemical preference of wild-type (WT) DFPase for the substrates sarin (GB), soman (GD), and cyclosarin (GF) was determined using a biological assay based on the inhibition of human acetylcholinesterase (AChE). The enzyme concentration was maintained at a dilute 20−30 nM depending on the substrate and enzyme mutant to ensure accurate sampling. For GF, 50% of the agent is hydrolyzed after 300 s, but virtually no detoxification has occurred. Only after 7500 s is complete degradation observed (Figure 1a). It was recently shown that the two enantiomers of GF possess markedly differing toxicities.[41] In the first phase of the reaction only the less toxic enantiomer is hydrolyzed while a substantial decrease in toxicity is only detected after prolonged reaction times. The same behavior is seen for GD while for GB there is no clear stereochemical preference. The results are in agreement with qualitative observations made by Schulz and co-workers.[10] It was shown previously that the more toxic stereoisomers of GB and GD are those with *S* configuration at the phosphorus atom (S_P).[8,42] On the basis of the structural determinants of the AChE active site,[43,44] it can be assumed that this is also true for GF.

In a second step all stereoisomers of GB, GD, and GF were docked into the active site of WT DFPase. The binding mode of the substrate in the active site has to fulfill two criteria to adopt a productive arrangement for reaction. First, the phosphoryl oxygen has to coordinate to the catalytic calcium ion for substrate activation. Second, the leaving group of the substrate must be oriented away from catalytic residue D229

(27) Hartleib, J.; Rüterjans, H. *Biochim. Biophys. Acta* **2001**, *1546*, 312–324.
(28) Worek, F.; Reiter, G.; Eyer, P.; Szinicz, L. *Arch. Toxicol.* **2002**, *76*, 523–529.
(29) Ellman, G. L.; Courtney, K. D.; Andres, V.; Feather-Stone, R. M. *Biochem. Pharmacol.* **1961**, *7*, 88–95.
(30) Worek, F.; Mast, U.; Kiderlen, D.; Diepold, C.; Eyer, P. *Clin. Chim. Acta* **1999**, *288*, 73–90.
(31) Eyer, P.; Worek, F.; Kiderlen, D.; Sinko, G.; Stuglin, A.; Simeon-Rudolf, V.; Reiner, E. *Anal. Biochem.* **2003**, *312*, 224–227.
(32) Hart, G. J.; O'Brien, R. D. *Biochemistry* **1973**, *12*, 2940–2945.
(33) Reiter, G.; Koller, M.; Thiermann, H.; Dorandeu, F.; Mikler, J.; Worek, F. *J. Chromatogr., B: Anal. Technol. Biomed. Life Sci.* **2007**, *859*, 9–15.
(34) Morris, G. M.; Goodsell, D. S.; Halliday, R. S.; Huey, R.; Hart, W. E.; Belew, R. K.; Olson, A. J. *J. Comput. Chem.* **1998**, *19*, 1639.
(35) Sanner, M. F. *J. Mol. Graphics Modell.* **1999**, *17*, 57.
(36) Sadowski, J.; Gasteiger, J. *Chem. Rev.* **1993**, *93*, 2567–2581.
(37) van der Spoel, D.; Lindahl, E.; Hess, B.; Groenhof, G.; Mark, A. E.; Berendsen, H. J. C. *J. Comput. Chem.* **2005**, *26*, 1701–1718.
(38) Hess, B.; Kutzner, C.; van der Spoel, D.; Lindahl, E. *J. Chem. Theory Comput.* **2008**, *4*, 435.
(39) van Gunsteren, W. F.; Billeter, S. R.; Eising, A. A.; Hünenberger, P. H.; Krüger, P.; Mark, A. E.; Scott, W. R. P.; Tironi, I. G. *Biomolecular Simulation: The Gromos 96 Manual and User Guide*; vdf Hochschulverlag: Zürich, Switzerland, 1996.
(40) Schuettelkopf, A. W.; van Aalten, D. M. F. *Acta Crystallogr., Sect. D: Biol. Crystallogr.* **2004**, *60*, 1355–1363.
(41) Harvey, S.; Kolakowski, J.; Cheng, T.; Rastogi, V.; Reiff, L. P.; DeFrank, J. J.; Raushel, F. M.; Hill, C. *Enzyme Microb. Technol.* **2005**, *37*, 547–555.
(42) Ordentlich, A.; Barak, D.; Kronman, C.; Benschop, H. P.; De Jong, L. P.; Ariel, N.; Barak, R.; Segall, Y.; Velan, B.; Shafferman, A. *Biochemistry* **1999**, *38*, 3055–3066.
(43) Albaret, C.; Lacoutière, S.; Ashman, W. P.; Froment, D.; Fortier, P. L. *Proteins* **1997**, *28*, 543–555.
(44) Shafferman, A.; Barak, D.; Stein, D.; Kronman, C.; Velan, B.; Greig, N. H.; Ordentlich, A. *Chem. Biol. Interact.* **2008**, *175*, 166–172.

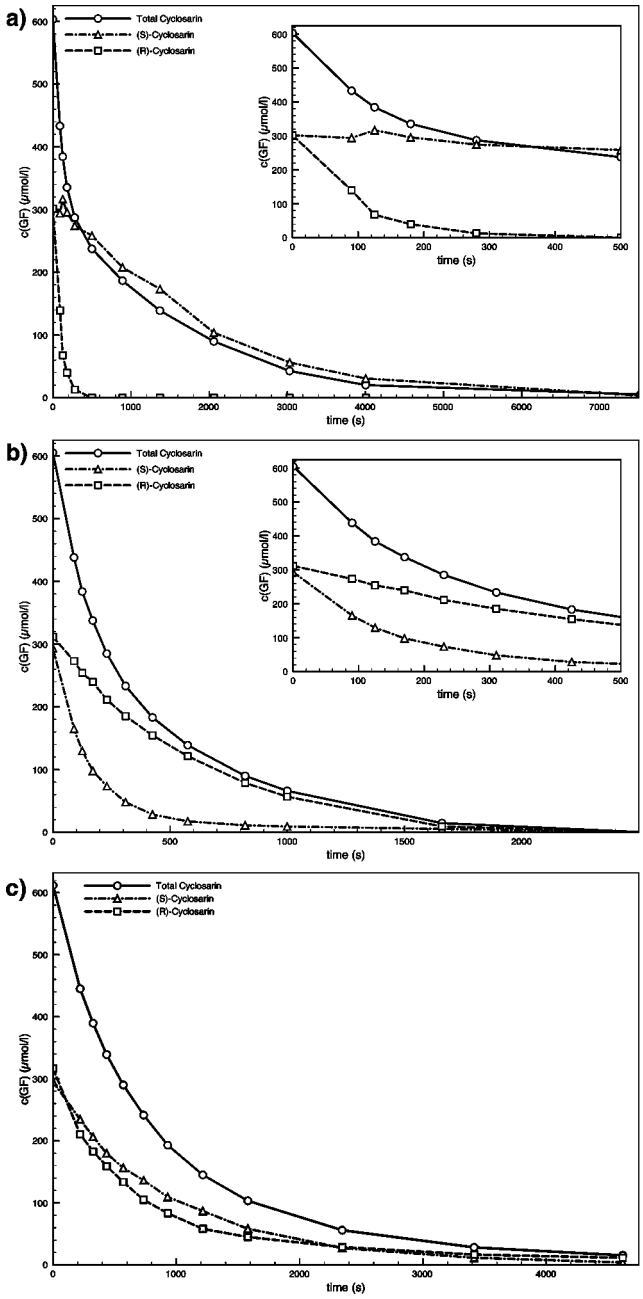

Figure 1. (a) Hydrolysis of enantiomers of GF by WT DFPase. (b) Hydrolysis of enantiomers of GF by Mut1. (c) Hydrolysis of enantiomers of GF by Mut2. (Data for substrates GB and GD can be found in the Supporting Information.)

in order to allow an in-line attack of the free D229 oxygen on the phosphorus.[5] The lowest energy orientations of the two enantiomers of GF bound to DFPase can be deduced from Figure 2. The figure shows (R_P)-GF in the active site of WT DFPase. Docking of (S_P)-GF shows a similar orientation but with the phosphorus-bound fluoride and methyl groups exchanged. An orientation that would allow a subsequent reaction can only be found for the less toxic R_P enantiomer of GF while the binding mode of the more toxic S_P enantiomer does not allow an in-line attack of D229 on the phosphorus atom. Similar results are obtained for the stereoisomers of GD while the small size of GB allows productive orientations for both enantiomers. This is in agreement with the results obtained using the biological assay.

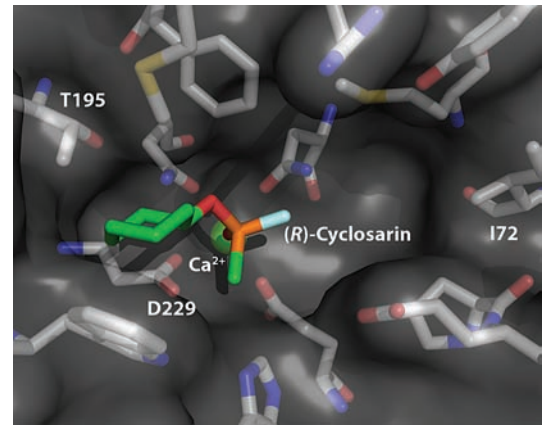

Figure 2. Docked orientation of (R_P)-GF in the active site of WT DFPase. Docking of (S_P)-GF shows a similar orientation but with the phosphorus-bound fluoride and methyl groups exchanged.

Rational Design of Enhanced DFPase Mutants. The DFPase active site is a quasisymmetrical elongated cleft with the catalytic calcium ion bound on the bottom of the binding pocket. One of the determinants for the binding orientation is the preference of the large alkoxy chain of the substrate to bind in either the left or the right side of the binding pocket (left, pointing toward T195; right, pointing toward I72). The docking reveals that in WT DFPase these side chains prefer the left side of the pocket. Therefore, our engineering efforts focused on limiting the space of the left side of the pocket forcing the alkoxy chain of the substrate to the right side by introducing a larger residue at position T195. The first reaction step in the catalytic cycle of DFPase is the attack of D229 on the substrate phosphorus atom. This leads to the formation of the phosphoenzyme intermediate. During the course of this first step a Walden inversion on the phosphorus atom takes place. This inversion is accompanied by movement and rearrangement of the substituents on the phosphorus atom, especially the large alkoxy group. To facilitate these movements a more open binding pocket was generated by removing steric constraints in the vicinity of the leaving group (E37, Y144, R146). The final quadruple mutant generated was E37A/Y144A/R146A/T195M (Mut1).

Structure and Activity of Designed DFPase Mutants. Mut1 and another mutant containing an aspartate at position 37 (E37D/Y144A/R146A/T195M; Mut2) were crystallized successfully and their crystal structures determined (PDB: 3HLH for Mut1, 3HLI for Mut2). Data collection and refinement statistics are shown in Table 1. Crystals of the two mutants grew in a previously uncharacterized space group ($P2_1$ compared to $P2_12_12_1$ for the WT), containing four molecules in the asymmetric unit. Nevertheless, structural comparison of WT DFPase (PDB: 1E1A) and the four mutant molecules in the asymmetric unit reveals only minor differences (0.2−0.3 Å rmsd), localized to loop regions and crystal contact areas. The Cβ atoms of the mutated amino acids in Mut1 (A37, A144, A146) superimpose with the Cβ atoms of the original side chains in the WT (E37, Y144, R146). Cβ and Cγ of the new side chain of M195 (formerly T195) can be superimposed with the Cβ and Cγ of the original side chain in the WT. This coincides with another observation made with structurally characterized mutants of DFPase: the protein backbone is highly resistant to structural changes upon side chain mutations. This feature of DFPase is especially useful for targeting specific mutations for rational design efforts. Despite the overall structural rigidity of the

Table 1. Data Collection and Refinement Statistics

	Mut1	Mut2
PDB code	3HLH	3HLI
source	ESRF ID-14, $\lambda = 0.933$ Å	ESRF BM16, $\lambda = 1.007$ Å
space group	$P2_1$	$P2_1$
unit cell	$a = 67.11$ Å $b = 74.39$ Å $c = 118.64$ Å $\beta = 99.9°$	$a = 66.95$ Å $b = 74.49$ Å $c = 118.95$ Å $\beta = 100.0°$
resolution	1.8 Å	1.4 Å
R_{sym}	0.136 (0.458)	0.053 (0.308)
$\langle I/\sigma(I)\rangle$	5.0 (1.6)	18.8 (4.4)
completeness	99.2% (98.7)	94.5% (86.3)
redundancy	3.8	3.1
indep reflections	105813 (incl 5332 for R_{free})	213535 (incl 10622 for R_{free})
R_{free}/R_{cryst}	0.218/0.195	0.221/0.205
rmsd bond lengths	0.005 Å	0.004 Å
rmsd bond angles	1.484°	1.455°
B-factor	11.3 Å^2	12.2 Å^2
outer shell	(1.90−1.80 Å)	(1.45−1.40 Å)

Table 2. Specific Enzymatic Activities of DFPase WT, Mut1, and Mut2 against 0.1% DFP, GB, GD, and GF

	WT	Mut1	Mut2
DFP (8.2 mM)[a]	247 ± 10[b]	390 ± 21	429 ± 21
sarin (GB, 14.3 mM)	110 ± 6	862 ± 32	418 ± 3
soman (GD, 11.0 mM)	82 ± 14	192 ± 8	117 ± 7
cyclosarin (GF, 10.0 mM)	198 ± 15	258 ± 13	143 ± 8

[a] Substrate concentrations in parentheses. [b] U/mg; 1 U = 1 μmol/min.

mutant structures, there is also one distinct difference relative to the WT. *B*-factors for residues in the loop region 141−151 of Mut1 and Mut2, which form part of the active site rim in DFPase, are elevated relative to the WT. This suggests a higher mobility of this loop in the mutants, which can be attributed to the two mutations in this region (Y144A, R146A). The replacement of the large arginine and tyrosine side chains by alanine reduces the contact area and removes torsional and steric restraints, increasing the plasticity of the DFPase active site.

Mut1 shows a pronounced preference for the more toxic S_P stereoisomers of GF (Figure 1b) as well as for GB and GD combined with a substantially enhanced enzymatic activity (Table 2). The preference of DFPase for the more toxic enantiomer of GF was also demonstrated by the use of a modified GC/MS assay with a chiral column that allows for the baseline separation of both enantiomers.[33] Compared to the indirect biological assay this method can directly visualize the disappearance of the two individual enantiomers. GF was hydrolyzed both with WT DFPase and Mut1, and samples were taken at intervals and subjected to chiral GC separation and MS detection. The more toxic *S*-(−)-GF eluted first and the less toxic *R*-(+)-GF second. WT DFPase prefers the less toxic stereoisomer leading to a faster degradation of this substrate (Figure 3a) while Mut1 prefers the more toxic stereoisomer (Figure 3b). Mut2 is slightly less active than Mut1, particularly in the case of GB where only half the specific activity of Mut1 is observed. Attempts to determine exact kinetic constants (K_M, k_{cat}) for the mutants with substrates GB, GD, and GF suffered from the low affinity of the substrates. Due to safety restrictions the maximum substrate concentration that could be used was 0.2% in the final reaction solution (approximately 10 mM). This is still below the K_M of Mut1 and Mut2 as at the maximum substrate concentration the reaction rate was still linearly dependent on the agent concentration and therefore $[S] \ll K_M$ (data not shown). Even though k_{cat} and K_M

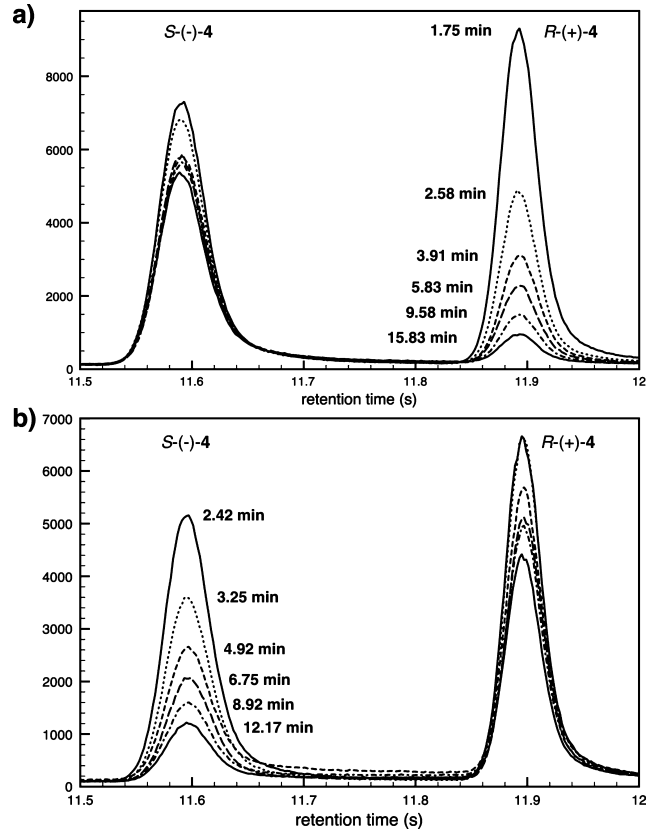

Figure 3. (a) Degradation of GF using WT DFPase monitored by chiral GC/MS showing the preference for less toxic *R*-(+)-GF. (b) Similar results for the degradation of GF using Mut1, showing preference for the more toxic *S*-(−)-GF.

cannot be determined individually under these conditions, it is still possible to determine k_{cat}/K_M if a single substrate is present. In the present case, however, the substrate stereoisomers act as substrates as well as competitive inhibitors of each other. Yeung et al. have presented a mathematical model for the determination of kinetic constants for the four stereoisomers of GD hydrolyzed by the enzyme paraoxonase.[15] The biological assay based on inhibition of AChE used in this study is only able to discriminate the pair of GD stereoisomers with a different configuration of the phosphorus atom, as this is the dominant stereocenter that determines toxicity, but is unable to individually detect all four steoroisomers. We have only used data for GB and GF (both with Mut1 and Mut2) to determine k_{cat}/K_M using a version of the mathematical model for GD/paraoxonase for a system with only one pair of enantiomers. k_{cat}/K_M for each GB and GF enantiomer was determined by computationally fitting the variables to the model equations and values are listed in Table 3.

Analyzing the k_{cat}/K_M values for GB, we can see that the values for both enantiomers of GB are almost identical in case of the wild type (ratio S/*R* = 0.89). Under the experimental conditions where $[S] \ll K_M$ it can be shown that the ratio of the k_{cat}/K_M values is equal to the ratio of the reaction rates of the two enantiomers if they are present at equal concentrations (as in the case of a racemic mixture). Both mutants show a preference for the more toxic (S_P)-GB, and this preference is more pronounced for Mut1. As can be seen from Table 3 this is achieved by an enhanced k_{cat}/K_M for (S_P)-GB and a decreased value for (R_P)-GB (ratio *S*/*R* Mut1 = 5.11; Mut2 = 2.96). In case of GF, the DFPase WT shows a distinct preference for the less toxic enantiomer (R_P)-GF (ratio S/*R* = 0.02, Figure 1a).

Table 3. k_{cat}/K_M for DFPase WT, Mut1, and Mut2 with Substrates DFP, GB, and GF and K_M and k_{cat} for Substrate DFP

		WT	Mut1	Mut2
DFP	K_M	3.76 ± 0.05 mM	2.12 ± 0.07 mM	3.93 ± 0.14 mM
	k_{cat}	211 ± 9 s^{-1}	291 ± 7 s^{-1}	376 ± 13 s^{-1}
	k_{cat}/K_M [a]	5.6×10^4 M^{-1} s^{-1}	1.4×10^5 M^{-1} s^{-1}	9.6×10^4 M^{-1} s^{-1}
(*R*)-GB	k_{cat}/K_M [b]	$4.7 \pm 0.6 \times 10^4$ M^{-1} s^{-1}	$4.5 \pm 0.4 \times 10^4$ M^{-1} s^{-1}	$2.4 \pm 0.1 \times 10^4$ M^{-1} s^{-1}
ratio *S*/*R*		0.89	5.11	2.96
(*S*)-GB	k_{cat}/K_M [b]	$4.2 \pm 1.2 \times 10^4$ M^{-1} s^{-1}	$2.3 \pm 0.3 \times 10^5$ M^{-1} s^{-1}	$7.1 \pm 0.6 \times 10^4$ M^{-1} s^{-1}
(*R*)-GF	k_{cat}/K_M [b]	$7.2 \pm 1.6 \times 10^5$ M^{-1} s^{-1}	$1.3 \pm 0.1 \times 10^5$ M^{-1} s^{-1}	$2.7 \pm 0.4 \times 10^4$ M^{-1} s^{-1}
ratio *S*/*R*		0.02	3.77	0.89
(*S*)-GF	k_{cat}/K_M [b]	$1.7 \pm 0.5 \times 10^4$ M^1 s^{-1}	$4.9 \pm 0.3 \times 10^5$ M^{-1} s^{-1}	$2.4 \pm 0.2 \times 10^4$ M^{-1} s^{-1}

[a] Determined by direct calculation from K_M and k_{cat} (K_M and k_{cat} determined from at least three independent experiments). [b] Determined by fitting k_{cat}/K_M for both enantiomers (determined from at least three independent experiments).

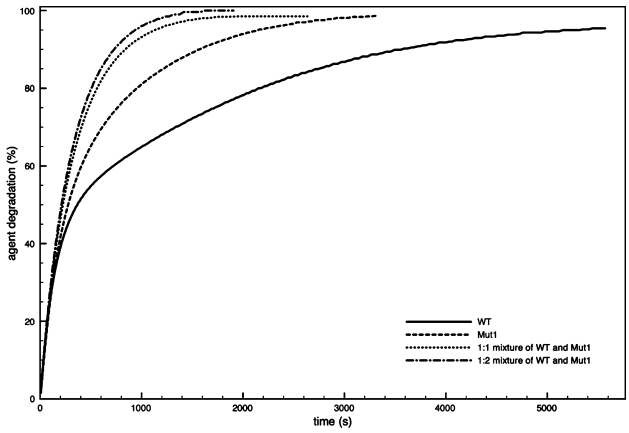

Figure 4. Degradation of GF using WT DFPase, Mut1, and mixtures (1:2 and 1:1 of WT and Mut1).

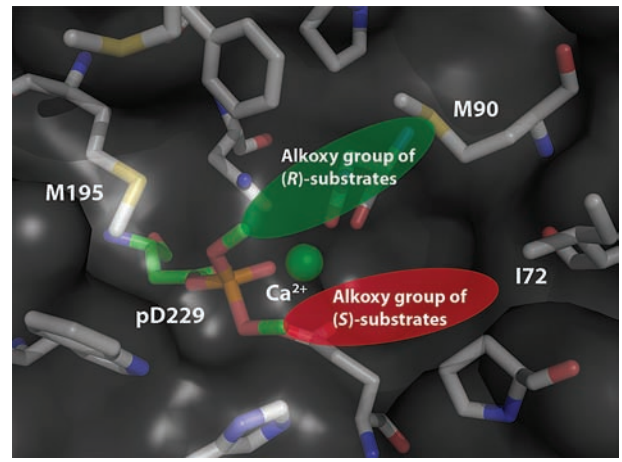

Figure 5. Model depicting the preferred orientation of the substrate alkoxy groups for the phosphoenzyme intermediate in the binding site of Mut1. The phosphorus-bound methyl group takes the position of an alkoxy oxygen atom (omitted for clarity).

This preference is reversed in the case of Mut1 (ratio S/*R* = 3.77, Figure 1b), but in the case of Mut2 both enantiomers are hydrolyzed with almost the same preference (ratio S/*R* = 0.89, Figure 1c).

WT DFPase and Mut1, both acting on the same chiral substrates, not only show reversed enantioselectivity but also have very different k_{cat} and K_M values. While the WT displays a lower K_M value compared to Mut1, which is important for agent degradation at very low substrate concentrations, it is clearly inferior in terms of k_{cat}, which determines the maximum achievable reaction rate of the enzyme. Thus, Mut1 is preferred at higher substrate concentrations, where its preference for the toxic enantiomers and the higher k_{cat} will lead to rapid detoxification. At lower substrate concentrations, the WT is preferred, due to the better K_M of the WT enzyme. To investigate this issue, WT and Mut1 as well as 1:1, 1:2, and 2:1 mixtures (with the same total enzyme content) were used to completely hydrolyze a solution of 660 μM GF (Figure 4). The biphasic hydrolysis curve for the WT is clearly visible. Although the K_M of Mut1 is much higher than the K_M of WT, the use of Mut1 reduces the required time for hydrolysis by more than 50%. Using mixtures of WT and Mut1 reduces the reaction time even further, but apparently the effect of the ratio is minimal in the range 1:2−2:1 (the 2:1 curve was omitted from Figure 3 for clarity but is virtually superimposable to that of the 1:1 mixture). These results clearly show that addition of DFPase WT to Mut1 partially overcomes the effect of the unfavorable K_M of Mut1 at low substrate concentrations.

With the structures of both mutants available, docking was used again to investigate the binding orientations of the stereoisomers of GB, GD, and GF, but the results were inconclusive regarding a distinct preference for the "left" and "right" side of the binding pocket compared to the WT. To find out which mutational site mainly contributes to the reversed enantioselectivity of the Mut1 the single mutants T195M and E37A and the double mutant Y144A/R146A were generated and tested with GF (see Supporting Information). None of these mutants displays the behavior of Mut1, although the preference for the less toxic enantiomers is less pronounced in T195M. Interestingly also E37A does not lead to a different selectivity compared to the WT. As shown above, Mut2 (containing the mutation E37D) only leads to an equal preference for both enantiomers in the case of GF, while Mut1 (containing mutation E37A) displays a reversed preference. To achieve the final selectivity of Mut1 all mutations are required. For DFPase this result can be explained structurally by modeling the different phosphoenzyme intermediates. In addition to the effect of T195 M introducing steric hindrance in the "left" side of the binding site, the other mutants open the pocket to facilitate the accommodation of the large alkoxy side chains of the substrates (Figure 5). It appears that the phosphoenzyme intermediate formed by the toxic S_P substrates is in an energetically more favorable conformation than those for the R_P substrates. Finally, the more open binding pocket should facilitate the structural rearrangements during the Walden inversion on the phosphorus atom that goes along with the nucleophilic attack by D229. Recent computational studies have revealed that this inversion does not have to occur in a

concerted manner but is also possible in a stepwise fashion.[45] Studies employing QM/MM methods are currently underway to gain a further understanding of the reaction step leading to the phosphoenzyme intermediate.

Discussion

A survey of the literature reporting engineering enantioselectivity in enzymes shows that rational design is still used but that evolutionary approaches tend to dominate the field. A class of enzymes where both approaches have been used are the lipases. Lipases are valuable enzymes for the creation of enantiomerically pure compounds, especially secondary alcohols, which are important building blocks in organic synthesis. Examples of a rational design approach include early work by Hirose et al.[46] focusing on the hydrolysis of 1,4-dihydropyridines and a more recent study by Magnusson et al.[47] focusing on secondary alcohols. Examples of evolutionary approaches can be found in the work of Zha et al.[48] using error prone PCR and DNA shuffling and Koga et al.[49] using single molecule PCR linked *in vitro* expression (SIMPLEX). These works show that both strategies can lead to enzyme variants with reversed enantioselectivity. Koga et al. point out, however, that improving activity or enantioselectivity by rational design remains challenging. The reasons for this are that the structural and functional effects of point mutations are not fully predictable and that site-directed mutagenesis is a slow and labor-intensive process such that only a limited number of variants can be produced and tested. Thus, evolutionary strategies are preferred if an assay for screening the mutant libraries exists that can be automated and used for high-throughput screening. Several examples with other enzymes using evolutionary methods can be found in the literature,[50−52] but also hybrid strategies have been reported, by using error prone PCR to generate libraries and point mutations to refine the initial hits from screening.[53]

Rational approaches require detailed knowledge about enzyme structure, substrate binding, and reaction mechanism. In the absence of this information, related enzymes with a highly conserved active site environment and similar but stereochemically reversed substrate specificity can be used as templates. This was demonstrated for vanillyl-alcohol oxidase (VAO) using a similar *p*-cresol methylhydroxylase (PCMH).[54] Analogously, the DFPase mutants reported in this study may be used to guide the engineering of the related enzyme paraxonase (PON).[13] Human PON1 has been considered as a catalytic *in vivo* scavenger. As the concentration of nerve agents is low in human plasma, even in cases of severe poisoning, a much smaller K_M is required for efficient enzyme activity than that displayed by WT DFPase and the mutants.[55]

The reason for choosing a rational design strategy for the engineering of DFPase was, as pointed out above, the toxic nature of the substrates that makes the screening of large mutant libraries virtually impossible. At the same time, substrate mimics, due to the presence of reporter groups and chromophores, are sometimes flawed surrogates for the real substrates. The creation of the DFPase mutants was aided by the wealth of structural data for the protein, detailed knowledge about the enzyme mechanism, and the unusual rigidity of the protein backbone, which helps to predict mutant structures and the effect of point mutations. It should be noted, however, that the rational design approach employed here is unlikely to generate an optimal enzyme mutant as the number of sampled mutants is still small compared to the large libraries used in evolutionary approaches.

Using rational design two quadruple mutants of DFPase have been constructed with a reversed enantioselectivity for G-type nerve agents. These mutants also display an enhanced enzymatic activity against the tested substrates. Both effects lead to a rapid detoxification of the reaction solution. Even though several articles in the literature deal with the enantioselectivity of nerve agent degrading enzymes like mammalian PON1[14−18] and PTE from *B. diminuta*,[56−59] they deal only with substrates mimicking the nerve agent, and only one PTE mutant with a reversed enantioselectivity against GF has been reported so far.[41] This was achieved by slowing down the turnover of the less toxic enantiomer resulting in a rather low overall activity. In contrast, the mutants reported here demonstrate an enhanced overall activity and enantioselectivity that allow for the practical use of DFPase for rapid detoxification. This highlights the significance of our findings and clearly shows that enzyme engineering efforts to enhance the activity and selectivity of DFPase are leading to promising results and that further optimizations seem feasible.

Acknowledgment. The German Ministry of Defense supported this work under contract E/UR3G/6G115/6A801. Part of this work was carried out by M. Melzer in partial fulfillment of the requirements for a medical doctoral degree at the Johannes Gutenberg University, Mainz, Germany. We thank the staff at ESRF for assistance with data collection. J.C.-H.C. was funded by the Hessian Ministry for Science and Culture.

Supporting Information Available: Detailed experimental procedures and supplementary results, including reaction curves for additional substrates and mutants as well as data to prove the accuracy of the analytical methods. This information is available free of charge via the Internet at http://pubs.acs.org.

JA905444G

(45) van Bochove, M. A.; Swart, M.; Bickelhaupt, F. M. *Phys. Chem. Chem. Phys.* **2009**, *11*, 259–267.
(46) Hirose, Y.; Kariya, K.; Nakanishi, Y.; Kurono, Y.; Achiwa, K. *Tetrahedron Lett.* **1995**, *36*, 1063–1066.
(47) Magnusson, A. O.; Takwa, M.; Hamberg, A.; Hult, K. *Angew. Chem., Int. Ed.* **2005**, *44*, 4582–4585.
(48) Zha, D.; Wilensek, S.; Hermes, M.; Jeager, K. E.; Reetz, M. T. *Chem. Commun.* **2001**, 2664–2665.
(49) Koga, Y.; Kato, K.; Nakano, H.; Yamane, T. *J. Mol. Biol.* **2003**, *331*, 585–592.
(50) May, O.; Nguyen, P. T.; Arnold, F. H. *Nat. Biotechnol.* **2000**, *18*, 317–320.
(51) Ivancic, M.; Valinger, G.; Gruber, K.; Schwab, H. *J. Biotechnol.* **2007**, *129*, 109–122.
(52) Bartsch, S.; Kourist, R.; Bornscheuer, U. T. *Angew. Chem., Int. Ed.* **2008**, *47*, 1508–1511.
(53) Williams, G. J.; Woodhall, T.; Farnsworth, L. M.; Nelson, A.; Berry, A. *J. Am. Chem. Soc.* **2006**, *128*, 16238–16247.
(54) van den Heuvel, R. H. H.; Fraaije, M. W.; Ferrer, M.; Mattevi, A.; van Berkel, W. J. H. *Proc. Natl. Acad. Sci. U.S.A.* **2000**, *97*, 9455–9460.
(55) Josse, D.; Lockridge, O.; Xie, W.; Bartels, C. F.; Schopfer, L. M.; Masson, P. *J. Appl. Toxicol.* **2001**, *21*, S7–S11.
(56) Chen-Goodspeed, M.; Sogorb, M. A.; Wu, F.; Hong, S. B.; Raushel, F. M. *Biochemistry* **2001**, *40*, 1325–1331.
(57) Chen-Goodspeed, M.; Sogorb, M. A.; Wu, F.; Raushel, F. M. *Biochemistry* **2001**, *40*, 1332–1339.
(58) Li, Y.; Aubert, S. D.; Raushel, F. M. *J. Am. Chem. Soc.* **2003**, *125*, 7526–7527.
(59) Hill, C. M.; Li, W. S.; Thoden, J. B.; Holden, H. M.; Raushel, F. M. *J. Am. Chem. Soc.* **2004**, *125*, 8990–8991.